Strain and Doping in Two-Dimensional SnTe Nanosheets: Implications for Thermoelectric Conversion

Fen Xiong[1,2], Hong Bin Tan[1], Chengliang Xia[1], and Yue Chen[1,2,*]

[1]Department of Mechanical Engineering, The University of Hong Kong, Pokfulam Road, Hong Kong SAR, China
[2]HKU Zhejiang Institute of Research and Innovation, 1623 Dayuan Road, Lin An 311305, China
*Corresponding author: yuechen@hku.hk

Abstract

Among thermoelectric materials, tin telluride has been attracting significant interest for its non-toxic and eco-friendly nature. Meanwhile, band engineering and ultra-thin film technologies have been reported to be promising in improving the performance of thermoelectric materials. In this work, we explore the potential of two-dimensional (2D) SnTe's thermoelectric performance, following the recent successful synthesis of 2D SnTe. It is found that pristine 2D SnTe is more likely to be a p-type semiconductor due to the existence of Sn vacancies. The electrical transport properties of 2D SnTe when it is (i) under compressive stress and (ii) doped with either nitrogen group or halogen group elements (including As, Sb, Bi, Br and I) have been studied from first-principles electronic structure calculations. Boltzmann transport study illustrates that equibiaxial compressive stress may enhance the electrical transport properties of 2D SnTe. Moreover, our calculations suggest that iodine and arsenic can be effective n-type and p-type dopants, respectively.

Keywords: Thermoelectric conversion; 2D SnTe; Nanosheets; Strain; Doping

Introduction

Despite the advancement of green energy generation, approximately two-thirds of the energy generated across the globe are wasted as unwanted heat [1]. Due to the increasing energy consumption, effectively converting waste heat into usable energy forms such as electricity are desperately needed. Thermoelectric materials have offered a possible solution to these issues - a type of materials that are able to convert heat into electricity directly without any mechanical means. The performance of a thermoelectric material is measured by how effective it can convert heat into electricity for a given temperature gradient. The performance and efficiency of thermoelectric materials can be measured by a dimensionless figure of merit, $ZT = \frac{S^2\sigma T}{\kappa}$, where S, σ, T, and κ represent the Seebeck coefficient, electrical conductivity, absolute temperature, and thermal conductivity, respectively.

Evidently, one would favor a high power factor (*PF*), which is defined as $S^2\sigma$, and a low thermal conductivity κ in a thermoelectric material that can give an overall high ZT value. Over the past few decades, bulk thermoelectric materials have been studied extensively and they generally have a positive correlation between electrical conductivity and thermal conductivity. Moreover, an enhancement in the Seebeck coefficient is usually followed by a decrease in electrical conductivity [2]. The resulting ZT value usually does not increase significantly as improving any of the parameters would adversely affect other transport properties. Various approaches such as nano-structuring [3], doping [4], and band engineering [5-6] have been used to enhance the value of *ZT*. It was reported that a record high *ZT* value of 2.6 exists at a working temperature of 923 K [7].

Ultra-thin films and 2D materials have been gaining attention for their unparalleled properties over bulk materials [2, 8-9]. Two-dimensional materials have been reported with various symmetry-breaking quantum phenomena including crystalline order [10], superconductivity [11], and charge density wave [12]. In some cases, the thermoelectric properties of 2D materials are better than those of their bulk phases [10]. For SnSe monolayer, the *ZT* peak value (3.27) was predicted to be seven times of that of the corresponding bulk phase at 700 K from density functional theory (DFT) [13]. In addition, it was found that the electrical conductivity and the thermal conductivity are negatively correlated in 2D SnS_2 and the *ZT* value can be enhanced by reducing the thickness of SnS_2 [14]. These results imply that 2D materials may achieve a higher thermoelectric performance.

Lead chalcogenides are widely known as high-performance thermoelectric materials [15-19]. However, lead based materials are not suitable for large-scale and commercial applications due to their toxicity. Meanwhile, tin based chalcogenides have also been gaining research attention for their non-toxic and more eco-friendly nature. Enhanced thermoelectric performance has been achieved in bulk SnTe [20]; fine tuning of the transport properties of bulk SnTe via doping [21] and nano-structuring [22] were proven to be effective in enhancing its thermoelectric efficiency. It was also predicted from theoretical calculations that 2D group IV chalcogenides can be dynamically stable [23]. Furthermore, atomic-thick SnTe films have been prepared on the graphitized 6H-SiC (0001) substrate under substrate temperature of 25 ~ 200 °C with the molecular beam epitaxial technique [24]. The successful fabrication of 2D SnTe motivates us to further investigate its thermoelectric properties.

For 2D materials, stress/strain engineering is an effective method to tune their properties such as ferroelectricity and thermoelectricity. The polarizations of 2D group-IV monochalcogenides have been reported to be linearly dependent on strain, and strain may induce ferroelectric phase transitions [25-26]. In our previous work, we have also reported that the non-ferroelectric phase of 2D lead chalcogenides can transform into a ferroelectric phase under equibiaxial in-plane tension [27-28]. Moreover, Morozova et al. have experimentally investigated the thermoelectric performance of quasi-two-dimensional titanium and zirconium trichalcogenides under high pressures [29].

In this work, we calculate the electrical transport properties of 2D SnTe based on DFT and Boltzmann transport theory. Our calculations indicate that the Seebeck coefficient and normalized electrical conductivity of 2D SnTe can be manipulated via an equibiaxial compressive stress to achieve a higher normalized power factor. On the other hand, pristine 2D SnTe is predicted to be likely a p-type semiconductor due to its crystallographic point defects. Doping is an important method to engineer the electronic structures and optimize the carrier concentration for a potentially higher thermoelectric performance. Our calculations also suggest that iodine and arsenic can be effective dopants for 2D SnTe.

Computational details

First-principles calculations were conducted using VASP [30]. The exchange-correlation effects were treated with the generalized gradient approximation of Perdew, Burke, and Ernzerhof [31]. The plane wave basis set was used to expand the electronic wave functions with a 500 eV cutoff energy. The convergence criterion for electrons was set to 10^{-5} eV. The Brillouin zone was sampled using the Γ-centered Monkhorst-Pack method with a density of $2\pi \times 0.03$ Å. The polarizations were calculated using the Berry phase method [32]. A 4 × 4 × 1 supercell containing 64 atoms was used to simulate point defects and the doped systems, for example: one Sn or Te atom was removed to simulate the vacancies; one Sn (Te) atom was replaced by a Te (Sn) atom to simulate the antisites; one Sn or Te atom was replaced by an impurity atom to simulate the doped systems. The same parameters, including the plane-wave cutoff energy, the convergence criteria and *k*-point density, were used for supercell and primitive cell calculations. To apply in-plane equibiaxial compressive stress to 2D SnTe, only the in-plane directions of the unit cell were relaxed using a modified version of VASP, in which selected components of the stress tensor can be set to zero during relaxation. To simulate 2D materials, a vacuum space with an approximately 20 Å thickness was introduced. The electrical transport properties were studied using the Boltzmann equations as implemented in BoltzTraP [33]. All crystal structures were fully relaxed.

Results and discussion

The thermoelectric properties of 2D SnTe with a $Pmn2_1$ space group are firstly investigated, and the results are shown in Fig. 1. Experimentally, Chang et al. have successfully synthesized atomic-thick SnTe. In our previous work, we have shown that 2D SnTe has a relative atomic displacement of about 0.12 Å along the *b* direction [27], which gives rise to a 1×10^{-10} C/m polarization [28]. To analyze the thermoelectric performance, the Seebeck coefficients, normalized electrical conductivities, and normalized power factors have been calculated using the Boltzmann equations. Although the lattice constants along *a* and *b* are different ($a = 4.56$ Å and $b = 4.57$ Å), the electrical transport properties along these directions are similar. Given the same carrier density (see Fig. 1(b, c and d)), it is predicted that the normalized electrical conductivity of p-type 2D SnTe is higher than that of n-type, but n-type 2D SnTe has a higher normalized power factor due to its higher absolute value of Seebeck coefficient. To study the origins of the differences in the electrical transport properties, the density of states (DOS) and band structure of 2D SnTe are calculated. It is observed from Fig. 1(e) that the DOS near the conduction band minimum is steeper than the DOS near the valence band maximum which may be related to the different degrees of band convergence (see Fig. 1(f)). According to the Mott's formula [34]:

$$S = \frac{\pi^2}{3}\frac{k_B^2 T}{e}\left[\frac{DOS(E)}{n(E)} + \frac{1}{\mu(E)}\frac{d\mu(E)}{dE}\right]\Big|_{E=E_F} \quad (1)$$

where n, $DOS(E)$, μ, E, and E_F are the concentration of carriers, the energy-dependent electronic density of states, mobility, energy of carriers, and Fermi level, respectively; therefore, an increase of DOS near Fermi level may lead to an enhancement of Seebeck coefficient.

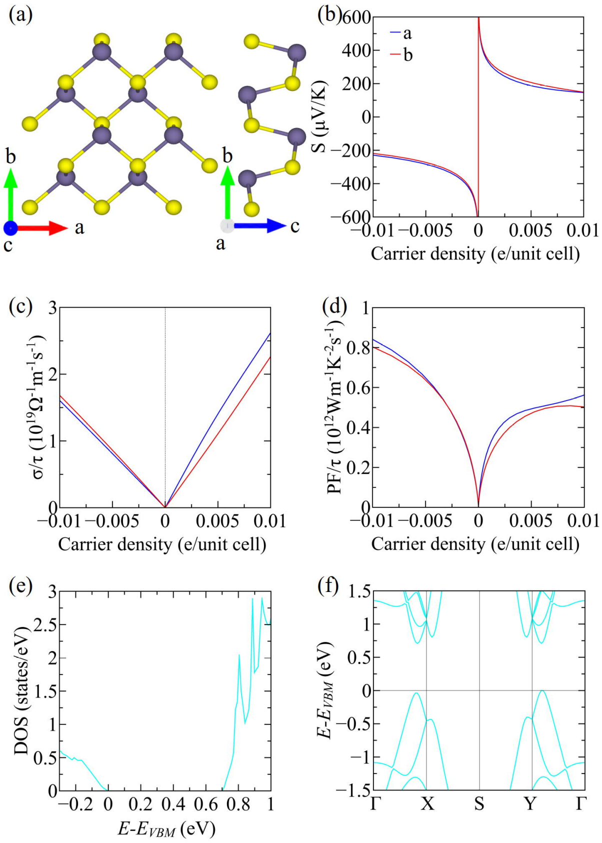

Fig. 1. The crystal structure (a), Seebeck coefficient (b), electrical conductivity (c) and power factor (d) normalized by the relaxation time τ at 300K, density of states (e), and band structure (f) of 2D SnTe. The valence band maximum has been shifted to 0 eV.

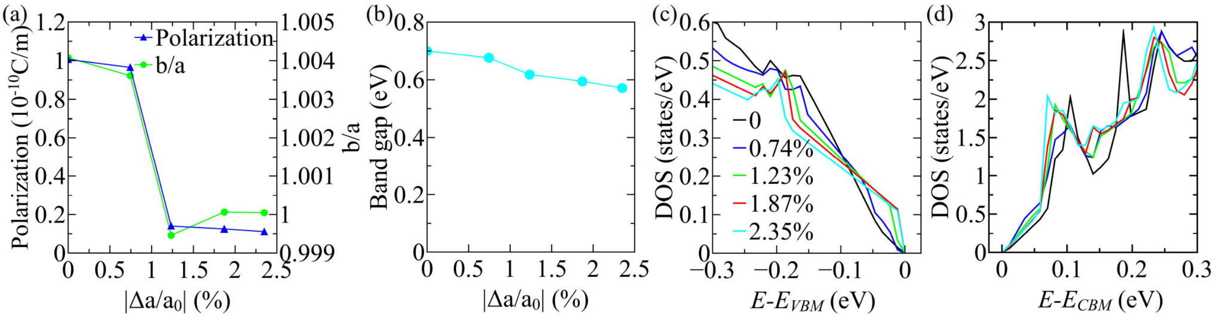

Fig. 2. The ferroelectric polarization, *b/a* ratio (a), and band gap (b) of 2D SnTe under different equibiaxial compressive stresses ($|\Delta a/a_0|$ represents the compressive strain along the *a* direction). (c, d) DOS of 2D SnTe under different equibiaxial compressive stresses (the number shown in panel (c) represents the different values of $|\Delta a/a_0|$); the valence band maximum (VBM) or the conduction band minimum (CBM) is shifted to zero.

To study the effects of equibiaxial compressive stress on the electronic structure and electrical transport properties of 2D SnTe, we have relaxed the unit cell of 2D SnTe under different equibiaxial compressive stresses. In Fig. 2(a), we present the ferroelectric polarization and the *b/a* ratio of 2D SnTe as a function of the compressive strain along the *a* direction ($|\Delta a/a_0|$). The polarization becomes approximately zero and the *b*/*a* ratio decreases to about one when the compressive strain ($|\Delta a/a_0|$) is larger than 1.2%. The results indicate that 2D SnTe has gone through a transition from the ferroelectric phase into a non-ferroelectric phase. The changes of the crystal structure under an equibiaxial compressive stress may result in a variation of its electronic structure. It is seen from Fig. 2(b-d) that the compressive stress enhances the DOS value near the band edges, while the band gap experiences a slight decrease.

To further study the effects of equibiaxial compressive stress on the electrical transport behaviors of 2D SnTe, we have performed Boltzmann transport calculations. In Fig. 3, the normalized power factors of n-type and p-type 2D SnTe, especially the former one, is found to be enhanced by compressive stress. Interestingly, both the absolute value of Seebeck coefficient and the normalized electrical conductivity of n-type 2D SnTe are improved under compression. The increase of Seebeck coefficient in n-type 2D SnTe under an equibiaxial compressive stress can be explained by the variation of DOS near the conduction band minimum and the Mott's formula. The increase of the normalized electrical conductivity may be related to the changes of band effective mass under compressive stress. Although our results suggest that equibiaxial compressive stress may be effective in enhancing the power factor of 2D SnTe, it should be noted that the relaxation time is not taken into account in the calculations.

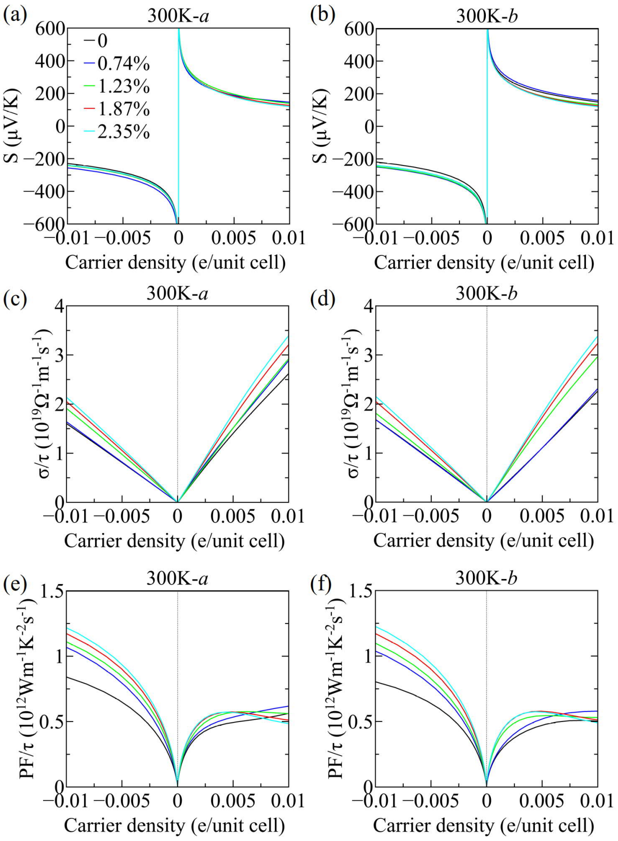

Fig. 3. Seebeck coefficient (a and b), electrical conductivity (c and d) and power factor (e and f) normalized by the relaxation time τ of 2D SnTe under different equibiaxial compressive stresses along directions *a* and *b* at 300 K. The number shown in panel (a) represents the different values of $|\Delta a/a_0|$.

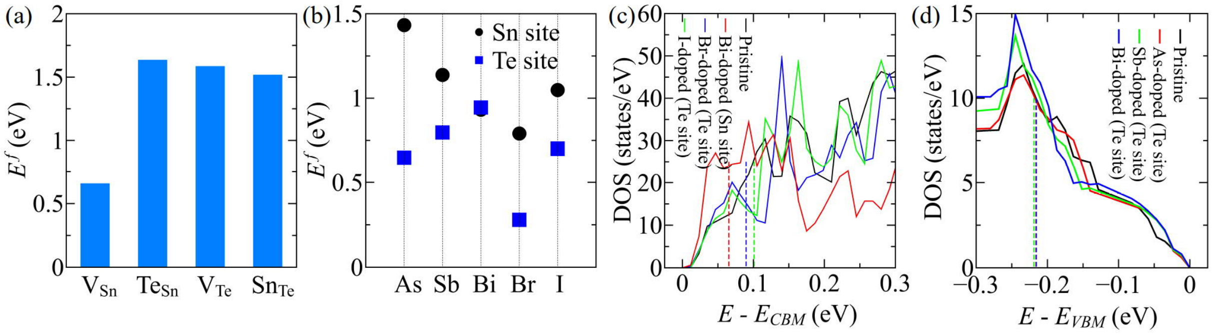

Fig. 4. (a) Formation energies of various point defects in 2D SnTe, including two types of vacancies (V_{Sn} and V_{Te}) and two types of antisites (Te_{Sn} and Sn_{Te}). (b) Formation energies of different doped 2D SnTe systems. (c) DOS of pristine, Bi-doped (Sn site), Br-doped (Te site), and I-doped (Te site) 2D SnTe; the conduction band minimum is shifted to zero. (d) DOS of pristine, As-doped (Te site), Sb-doped (Te site), and Bi-doped (Te site) 2D SnTe; the valence band maximum is shifted to zero. The vertical dashed lines represent the corresponding Fermi levels.

Point defects, which may be induced during the fabrication of 2D materials, are important factors affecting the electrical transport properties of semiconductors. Pristine SnTe in its bulk phase is a p-type semiconductor because of the presence of Sn vacancies [35]. To investigate the electrical transport properties of 2D SnTe, we have considered the different types of point defects, including vacancies (V_{Sn} and V_{Te}) and antisites (Te_{Sn} and Sn_{Te}). The formation energy of a point defect is calculated using the following equation:

$$E^f = E_{tot} - E_{perfect} - \sum_\alpha n_\alpha E_\alpha \tag{2}$$

where E_{tot} is the total energy of the supercell of 2D SnTe with a point defect; $E_{perfect}$ is the total energy of perfect 2D SnTe; n_α is the number of atoms removed from ($n_\alpha < 0$) or added to ($n_\alpha > 0$) the supercell, and E_α is the total energy of an atom in its bulk phase. Our DFT calculations indicate that Sn vacancy (V_{Sn}) has the lowest formation energy (see Fig. 4(a)); therefore, it is more likely to exist in 2D SnTe, which is in agreement with the experimental observations [22]. The existence of Sn vacancies suggests that pristine 2D SnTe is more likely to have p-type conduction. Doping has been widely used to engineer the electronic structures and tune the carrier concentrations of thermoelectric materials. In an attempt to obtain potentially higher thermoelectric performance of 2D SnTe, we investigate the doping effects of the nitrogen group (As, Sb and Bi) and the halogen group (Br and I) elements. For these dopants, their preferential substitutional sites are studied based on the calculations of formation energy as defined in Eq. 2. From Fig. 4(b), we observe that As and Sb tend to occupy the Te site, suggesting that they are potential p-type dopants for 2D SnTe. Br and I also tend to occupy the Te site, indicating that they are potential n-type dopants. Bi does not show an obvious site preference due to the small difference in the formation energies; thus, we have considered both cases when the Sn or Te site is occupied by Bi.

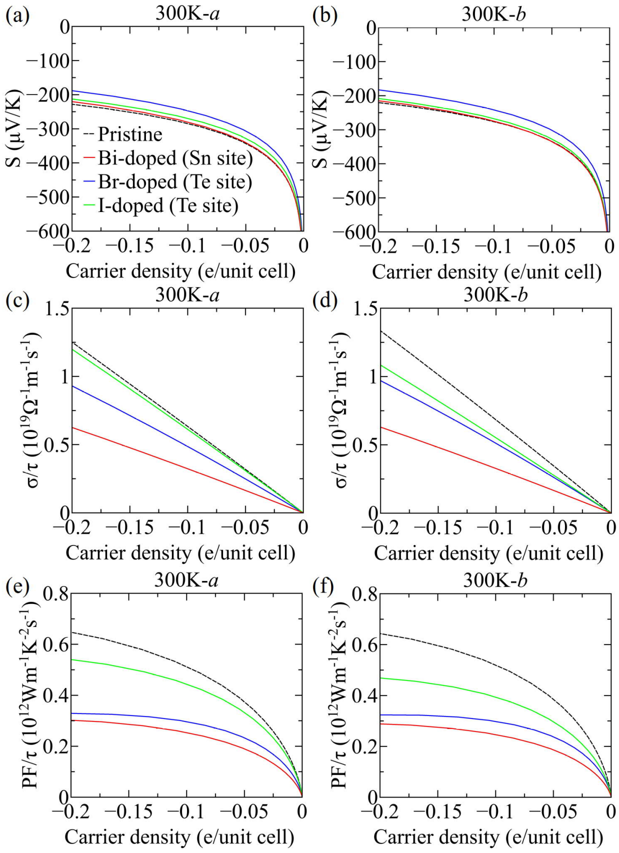

Fig. 5. Seebeck coefficient (a, b), normalized electrical conductivity (c, d), and normalized power factor (e, f) of n-type 2D SnTe at 300 K along the *a* and *b* directions. Results of pristine 2D SnTe calculated using a 4 × 4 × 1 supercell are shown for comparison.

To study the doping effects on the electronic structure, the DOS of the doped 2D SnTe have been calculated. As shown in Fig. 4(c), it is found that Bi (Sn site) enhances the DOS near the conduction band minimum, while I and Br have less significant effects on the DOS. In Fig. 4(d), it is seen that the nitrogen group elements only have minor effects on the valence band maximum of 2D SnTe. According to the Mott's formula, the Seebeck coefficient of 2D SnTe will be increased after Bi doping (Sn site). Furthermore, Boltzmann transport calculations have been conducted to investigate the doping effects on the electrical transport behaviors. For the n-type conduction (see Fig. 5), Bi-doped (Sn site) 2D SnTe has the largest Seebeck coefficient followed by I- and Br-doped 2D SnTe, in line with the expectation from DOS calculations. On the other hand, the normalized electrical conductivity of Bi-doped 2D SnTe is much lower than that of I-doped 2D SnTe comparing at the same carrier density. Hence, the normalized power factor of I-doped 2D SnTe is higher than those of the Br- and Bi-doped systems. For the p-type conduction (see Fig. 6), As-doped 2D SnTe has a higher normalized power factor than Sb-doped and Bi-doped 2D SnTe. It should be noted that impurity atoms in doped systems may induce additional scattering which could result in a change of the relaxation time, although it is predicted that I-doped and As-doped 2D SnTe may exhibit more promising electrical transport properties.

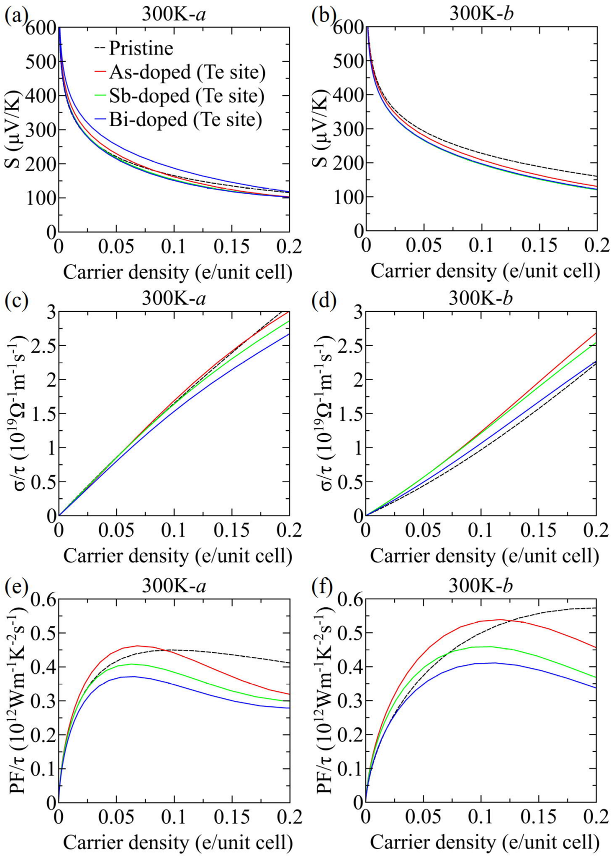

Fig. 6. Seebeck coefficient (a, b), normalized electrical conductivity (c, d), and normalized power factor (e, f) of p-type 2D SnTe at 300 K along the *a* and *b* directions. Results of pristine 2D SnTe calculated using a 4 × 4 × 1 supercell are shown for comparison.

Conclusions

The electronic structure and electrical transport properties of 2D SnTe have been calculated from first principles. Equibiaxial compressive stress is found to modify the electronic states near the Fermi level, and the changes in the electronic structure lead to an improvement of the normalized power factor. Furthermore, it is found that Sn vacancy is more likely to exist in 2D SnTe, resulting in p-type conduction. In an attempt of doping 2D SnTe for potentially higher electrical transport properties, elements As, Sb, Bi, Br, and I have been studied. It is found that I and As are more promising in achieving high normalized power factors in n-type and p-type 2D SnTe, respectively. This work is expected to stimulate further experimental studies on the engineering of the electronic structures and thermoelectric transport properties of 2D materials.

Supporting Information

Computational details of the electronic relaxation time, the optimized lattice parameters of the supercells of doped 2D SnTe, scattering rate and the electrical transport properties of 2D SnTe; phonon dispersions, band structures and density of states of 2D SnTe under compression; effective band structures of doped 2D SnTe.

Acknowledgement

We acknowledge the supports from the Research Grants Council of Hong Kong (grant nos: 17200017 and 17300018) and the National Natural Science Foundation of China (grant nos: 51706192 and 11874313). All calculations were performed using the research computing facilities offered by ITS, HKU.

References

1. Chu, S.; Majumdar, A. Opportunities and challenges for a sustainable energy future. *Nature* **2012,** *488*, 294-303.
2. Hicks, L.; Dresselhaus, M. S. Thermoelectric figure of merit of a one-dimensional conductor. *Phys. Rev. B* **1993,** *47*, 16631-16634.
3. Li, J. F.; Liu, W. S.; Zhao, L. D.; Zhou, M. High-performance nanostructured thermoelectric materials. *NPG Asia Mater.* **2010,** *2*, 152-158.
4. Kaur, K.; Kumar, R. Enhancement of figure of merit(ZT) by doping Bi in Mg_2Si for energy harvesting applications. *Prog. Nat. Sci. Mater.* **2017,** *26*, 533-539.
5. Pei, Y. Z.; Wang, H.; Snyder, G. J. Band engineering of thermoelectric materials. *Adv. Mater.* **2012,** *24*, 6125-6135.
6. Lv, H. Y.; Lu, W. J.; Shao, D. F.; Sun, Y. P. Enhanced thermoelectric performance of phosphorene by strain-induced band convergence. *Phys. Rev. B* **2014,** *90*, 085433.
7. Zhao, L. D.; Lo, S.; Zhang, Y.; Sun, H.; Tan, G.; Uher, C.; Wolverton, C.; Dravid, V. P.; Kanatzidis, M. G. Ultralow thermal conductivity and high thermoelectric figure of merit in SnSe crystals. *Nature* **2014,** *508*, 373.
8. Beyer, H.; Nurnus, J.; Böttner, H.; Lambrecht, A.; Wagner, E.; Bauer, G. High thermoelectric figure of merit ZT in PbTe and Bi_2Te_3-based superlattices by a reduction of the thermal conductivity. *Physica E* **2002,** *13*, 965-968.
9. Hung, N. T.; Nugraha, A. R. T.; Saito, R. Two-dimensional InSe as a potential thermoelectric material. *Appl. Phys. Lett.* **2017,** *111*, 092107.
10. Novoselov, K. S.; Geim, A. K.; Morozov, S.; Jiang, D.; Katsnelson, M. I.; Grigorieva, I. V.; Dubonos, S. V.; Firsov, A. A. Two-dimensional gas of massless Dirac fermions in graphene. *Nature* **2005,** *438*, 197.
11. Gozar, A.; Logvenov, G.; Kourkoutis, L. F.; Bollinger, A. T.; Giannuzzi, L. A.; Muller, D. A.; Bozovic, I. High-temperature interface superconductivity between metallic and insulating copper oxides. *Nature* **2008,** *455*, 782.
12. Barja, S.; Wickenburg, S.; Liu, Z.; Zhang, Y.; Ryu, H.; Ugeda, M. M.; Hussain, Z.; Shen, Z.; Mo, S.; Wong, E. Charge density wave order in 1D mirror twin boundaries of single-layer $MoSe_2$. *Nat. Phys.* **2016,** *12*, 751-756.
13. Wang, F. Q.; Zhang, S.; Yu, J.; Wang, Q. Thermoelectric properties of single-layered SnSe sheet. *Nanoscale* **2015,** *7*, 15962-15970.
14. Lee, M. J.; Ahn, J. H.; Sung, J. H.; Heo, H.; Jeon, S. G.; Lee, W.; Song, J. Y.; Hong, K. H.; Choi, B.; Lee, S. H. Thermoelectric materials by using two-dimensional materials with negative correlation between electrical and thermal conductivity. *Nat. Commun.* **2016,** *7*, 12011.
15. Hsu, K. F.; Loo, S.; Guo, F.; Chen, W.; Dyck, J. S.; Uher, C.; Hogan, T.; Polychroniadis, E.; Kanatzidis, M. G. Cubic $AgPb_mSbTe_{2+m}$: bulk thermoelectric materials with high figure of merit. *Science* **2004,** *303*, 818-821.

16. Biswas, K.; He, J.; Blum, I. D.; Wu, C.-I.; Hogan, T. P.; Seidman, D. N.; Dravid, V. P.; Kanatzidis, M. G. High-performance bulk thermoelectrics with all-scale hierarchical architectures. *Nature* **2012,** *489*, 414.
17. Heremans, J. P.; Jovovic, V.; Toberer, E. S.; Saramat, A.; Kurosaki, K.; Charoenphakdee, A.; Yamanaka, S.; Snyder, G. J. Enhancement of thermoelectric efficiency in PbTe by distortion of the electronic density of states. *Science* **2008,** *321*, 554-557.
18. Bourgès, C.; Gilmas, M.; Lemoine, P.; Mordvinova, N. E.; Lebedev, O. I.; Hug, E.; Nassif, V.; Malaman, B.; Daou, R.; Guilmeau, E. Structural analysis and thermoelectric properties of mechanically alloyed colusites. *J. Mater. Chem. C* **2016,** *4*, 7455-7463.
19. Zhao, L.; Dravid, V. P.; Kanatzidis, M. G. The panoscopic approach to high performance thermoelectrics. *Energy Environ. Sci.* **2014,** *7*, 251-268.
20. Tan, X.; Shao, H.; He, J.; Liu, G.; Xu, J.; Jiang, J.; Jiang, H. Band engineering and improved thermoelectric performance in M-doped SnTe (M= Mg, Mn, Cd, and Hg). *Phys. Chem. Chem. Phys.* **2016,** *18*, 7141-7147.
21. Zhou, M.; Gibbs, Z. M.; Wang, H.; Han, Y.; Li, L.; Snyder, G. J. Thermoelectric performance of Co-doped SnTe with resonant levels. *Appl. Phys. Lett.* **2016,** *109*, 042102.
22. Zhang, Q.; Liao, B.; Lan, Y.; Lukas, K.; Liu, W.; Esfarjani, K.; Opeil, C.; Broido, D.; Chen, G.; Ren, Z. High thermoelectric performance by resonant dopant indium in nanostructured SnTe. *Proc. Natl. Acad. Sci. U.S.A.* **2013,** *110*, 13261-13266.
23. Singh, A. K.; Hennig, R. G. Computational prediction of two-dimensional group-IV mono-chalcogenides. *Appl. Phys. Lett.* **2014,** *105*, 042103.
24. Chang, K.; Liu, J.; Lin, H.; Wang, N.; Zhao, K.; Zhang, A.; Jin, F.; Zhong, Y.; Hu, X.; Duan, W. Discovery of robust in-plane ferroelectricity in atomic-thick SnTe. *Science* **2016,** *353*, 274-278.
25. Fei, R.; Li, W.; Li, J.; Yang, L. Giant piezoelectricity of monolayer group IV monochalcogenides: SnSe, SnS, GeSe, and GeS. *Appl. Phys. Lett.* **2015,** *107*, 173104.
26. Fei, R.; Kang, W.; Yang, L. Ferroelectricity and phase transitions in monolayer group-IV monochalcogenides. *Phys. Rev. Lett.* **2016,** *117*, 097601.
27. Zhang, X.; Yang, Z.; Chen, Y. Novel two-dimensional ferroelectric PbTe under tension: A first-principles prediction. *J. Appl. Phys.* **2017,** *122*, 064101.
28. Xiong, F.; Zhang, X.; Lin, Z.; Chen, Y. Ferroelectric engineering of two-dimensional group-IV monochalcogenides: The effects of alloying and strain. *J Materiomics.* **2018,** *4*, 139-143.
29. Morozova, N. V.; Korobeinikov, I. V.; Kurochka, K. V.; Titov, A. N.; Ovsyannikov, S. V. Thermoelectric Properties of Compressed Titanium and Zirconium Trichalcogenides. *J. Phys. Chem. C* **2018,** *122*, 14362-14372.
30. Kresse, G.; Furthmüller, J. Efficient iterative schemes for ab initio total-energy calculations using a plane-wave basis set. *Phys. Rev. B* **1996,** *54*, 11169-11186.
31. Perdew, J. P.; Burke, K.; Ernzerhof, M. Generalized gradient approximation made simple. *Phys. Rev. Lett.* **1996,** *77*, 3865-3868.
32. King-Smith, R. D.; Vanderbilt, D. Theory of polarization of crystalline solids. *Phys. Rev. B* **1993,** *47*, 1651.
33. Madsen, G. K.; Singh, D. J. BoltzTraP. A code for calculating band-structure dependent quantities. *Comput. Phys. Commun.* **2006,** *175*, 67-71.
34. Rowe, D. M., *CRC Handbook of Thermoelectrics*. CRC-Press: 1995.

35. Wang, N.; West, D.; Liu, J.; Li, J.; Yan, Q.; Gu, B.; Zhang, S. B.; Duan, W. Microscopic origin of the p-type conductivity of the topological crystalline insulator SnTe and the effect of Pb alloying. *Phys. Rev. B* **2014,** *89*, 045142.